Carcinogenesis vol.34 no.7 pp.1558–1566, 2013
doi:10.1093/carcin/bgt066
Advance Access publication February 21, 2013

Piper betel leaf extract: anticancer benefits and bio-guided fractionation to identify active principles for prostate cancer management

Rutugandha Paranjpe[1,†], Sushma R.Gundala[1,†], N.Lakshminarayana[1,2], Arpana Sagwal[2], Ghazia Asif[3], Anjali Pandey[4] and Ritu Aneja[1,*]

[1]Department of Biology and [2]Department of Chemistry, Georgia State University, Atlanta, GA 30303, USA, [3]Department of Human Genetics, Emory University School of Medicine, Atlanta, GA 30322, USA and [4]Indian Institute of Integrative Medicine (CSIR), Jammu, India

*To whom correspondence should be addressed. Tel: +1-404-413-5417; Fax: +1-404-413-530;
Email: raneja@gsu.edu

Plant extracts, a concoction of bioactive non-nutrient phytochemicals, have long served as the most significant source of new leads for anticancer drug development. Explored for their unique medicinal properties, the leaves of *Piper betel*, an evergreen perennial vine, are a reservoir of phenolics with antimutagenic, antitumor and antioxidant activities. Here, we show that oral feeding of betel leaf extract (BLE) significantly inhibited the growth of human prostate xenografts implanted in nude mice compared with vehicle-fed controls. To gain insights into the 'active principles', we performed a bioactivity-guided fractionation of methanolic BLE employing solvents of different polarity strengths using classical column chromatography. This approach yielded 15 fractions, which were then pooled to 10 using similar retention factors on thin-layer chromatographs. Bioactivity assays demonstrated that one fraction in particular, F2, displayed a 3-fold better *in vitro* efficacy to inhibit proliferation of prostate cancer cells than the parent BLE. The presence of phenols, hydroxychavicol (HC) and chavibetol (CHV), was confirmed in F2 by nuclear magnetic resonance, high-performance liquid chromatography and mass spectroscopy. Further, the HC containing F2 subfraction was found to be ~8-fold more potent than the F2 subfraction that contained CHV, in human prostate cancer PC-3 cells as evaluated by the 3-(4,5-dimethylthiazole-2-yl)-2,5-diphenyl tetrazolium bromide assay. Removing CHV from F2 remarkably decreased the IC_{50} of this fraction, indicating that HC is perhaps the major bioactive constituent, which is present to an extent of 26.59% in BLE. These data provide evidence that HC is a potential candidate for prostate cancer management and warrants further preclinical evaluation.

Introduction

Demographic studies have reported discernible variations in prostate cancer incidence across the globe. Known to be one of the deadliest diseases, its mortality rate is higher in Westerners compared with Asians (1). Given the long latency of prostate cancer, it is believed that, although the disease initiates concurrently among these cultures, its progression is much slower compared with the western population. Such ethnic disparities have been reportedly linked to differences in dietary regimens that impart both chemotherapeutic and preventive benefits (2). Indisputable evidence indicates that a diet rich in lycopenes, legumes, cruciferous vegetables, curcumin and gingerols has been associated with a reduced risk of prostate cancer (3).

Fruits, vegetables and spices, with their antioxidant and detoxifying properties, can revert and delay the progression of prostate cancer mainly due to their abundance in polyphenols that offer multifarious health-promoting benefits (3–8). Polyphenols have been reported to be highly effective in fighting various chronic diseases like diabetes and cancer. Recent years have indeed witnessed a revival of interest in plant phytochemicals, especially polyphenols, as potential chemopreventive and chemotherapeutic agents. Intriguingly, the redox moieties of these compounds display a two-pronged approach to confer their unique 'dual ability' (9). Although the chemopreventive efficacy at low concentrations in normal cells is due to these compounds' antioxidant properties (9), other species of polyphenols can act as prooxidants at higher concentrations in cancer cells and generate reactive oxygen species, further inducing DNA damage and eventually apoptosis, thereby acting as potential chemotherapeutic agents (9). The relative natural abundance of polyphenols and their specificity toward cancer cells and thus lack of side effects have generated tremendous interest in these versatile molecules, emphasizing their advantages over traditional anticancer drugs (5).

Although these phytochemicals exist in leaf, root or bark as a complex mixture offering chemical diversity, their relative abundance is influenced by a number of factors such as environmental conditions, cultivation, time of collection, means of extraction, etc. (10,11). Since the content of pharmacologically active constituents may vary among crude extracts, it is imperative to identify the bioactive compounds as well as establish their optimum concentrations for maximum therapeutic activity (10,12). Isolation of these bioactive constituents and optimization of their effective concentrations would result in enhanced bioavailability, pharmacokinetics and thus efficacy (in comparison with their respective crude extracts). For example, the major components of *Curcuma longa* (commonly referred to as turmeric) are curcumin, demethoxycurcumin and bisdemethoxy curcumin. Extensive studies have revealed the enhanced efficacy of curcumin thus potentiating its use as an anticancer agent (13). No wonder curcumin, capsaicin and gingerols derived from the spices turmeric, red chili and ginger, respectively, have entered clinical trials as potential anticancer agents (14).

Piper betel leaves (*Piper betel* Linn.), also referred to as 'green gold' (15), are widely consumed as a condiment in Africa and Asia (especially India and Taiwan). The medicinal properties of *P.betel* can be traced back to ancient Vedic literature. Rich in phenols and terpenes, these leaves have been reported to exhibit antioxidant, anti-inflammatory, immunomodulatory and antitumor activities (16–18). Here, we report the previously unknown benefits of betel leaves in prostate cancer and a systematic fractionation of the leaf extract to identify the active principles. This study presents the first identification of the anticancer attributes of betel leaf extract (BLE) in inhibiting prostate cancer growth in mice models and emphasizes hydroxychavicol (HC) as a major contributor of its *in vitro* and *in vivo* efficacy in prostate cancer models.

Materials and methods

Cell culture, chemicals and reagents

Piper betel leaves were purchased from the local farmer's market in Atlanta, GA. Hexanes, ethyl acetate, dichloromethane and methanol were obtained from Fisher Scientific (Houston, TX). The silica used for classical chromatography was from EMD Biosciences. Thin-layer chromatography (TLC) plates were from EMD chemicals (Billerica, MA). PC-3, DU145 and 22RV1 prostate cancer cells were cultured in RPMI-1640 medium supplemented with 10% heat-inactivated fetal bovine serum and 5% penicillin/streptomycin. The normal prostate epithelial RWPE-1 cells were

Abbreviations: APC, allylpyrocatechol; BLE, betel leaf extract; CHV, chavibetol; DMSO, dimethyl sulfoxide; EU, eugenol; HC, hydroxychavicol; HPLC, high-performance liquid chromatography; IC_{50}, half-maximal inhibitory concentration; MS, mass spectrometry; MTT, 3-(4,5-dimethylthiazole-2-yl)-2,5-diphenyl tetrazolium bromide; NMR, nuclear magnetic resonance; PBS, phosphate-buffered saline; TLC, thin-layer chromatography; UV, ultraviolet.

[†]These authors contributed equally to this work.

cultured in Keratinocyte-SFM medium kit (Invitrogen, Grand Island, NY) supplemented with 10% heat-inactivated fetal bovine serum. Luciferase-expressing PC-3 cells (PC-3-luc) were from Calipers (Hopkinton, MA) and were maintained in minimum essential medium with 10% fetal bovine serum (Hyclone, Pittsburgh, PA). The 3-(4,5-dimethylthiazole-2-yl)-2,5-diphenyl tetrazolium bromide (MTT) dye (98% TLC), eugenol (EU), dimethyl sulfoxide (DMSO) and preparative TLC plates were from Sigma (St Louis, MO). HC was extracted from betel leaves and was characterized for >99% purity.

Preparation of methanolic BLE

Freshly cut betel leaves were lyophilized to remove any moisture present. Freeze-dried leaves were soaked in methanol overnight for three consecutive days. The supernatant was collected daily, concentrated under reduced pressure and lyophilized to remove any traces of moisture. The dried BLE was then stored at −80°C. Batch-to-batch variation was assessed by quantitating HC content via high-performance liquid chromatography (HPLC)-ultraviolet (UV) analysis, and no significant variations were observed in the three batches processed.

In vivo tumor growth and bioluminescent imaging

PC-3-luc cells (1×10^6) were subcutaneously injected on either flank of 6-week-old male BALB/c nude mice (Harlan Laboratories, Indianapolis, IN). When tumors were palpable, mice were randomly divided into four groups of five mice each. Control group received vehicle [phosphate-buffered saline (PBS) with 0.05% Tween-80, pH 7.4] and the three treatment groups received 200, 400 and 650 mg/kg body weight BLE dissolved in PBS with 0.05% Tween-80 (pH 7.4) by oral gavage daily. Tumor growth was monitored by measuring the luciferase activity in live mice by bioluminescent imaging in real-time using the IVIS *in vivo* imaging system (Caliper Life Sciences, Alameda, CA) with the Live Imaging software. Briefly, mice anesthetized with isoflurane were intraperitoneally injected 25 mg/ml luciferin and imaged with a CCD camera. An integration of 20 s with four binnings of 100 pixels was used for image acquisition. The relative photon quantitation at the tumor site of the mice from vehicle- or BLE-treated groups was quantitated twice a week for 6 weeks. All animal experiments were performed in compliance with Institutional Animal Care and Use Committee guidelines.

Immunofluorescence and immunohistochemical staining of tumor tissue

Paraffin-embedded tumor sections from vehicle- and BLE-treated groups were processed and immunostained with apoptotic markers, cleaved caspase-3 and cleaved poly (ADP ribose) polymerase, the proliferation marker, Ki67, and hematoxylin and eosin. Briefly, tumor tissues excised from the BLE and vehicle-treated mice were fixed in 10% formalin. The fixed tissues were embedded and sectioned into 4–5 µm thick slices. Formalin-fixed sections were subjected to sequential washing with xylene, 100% ethanol, 95% ethanol, 80% ethanol and H_2O for 3 min each. For antigen retrieval, slides incubating in 0.1 mol/l of sodium citrate in dH_2O (pH 6.0) were heated in a steam cooker for 10 min. After washing with PBS, slides were blocked with 5% bovine serum albumin in PBS, 0.1% Triton X-100 for 1 h at room temperature, followed by incubation with primary antibodies in blocking solution overnight at 4°C. After washing twice with PBS, slides for immunofluorescence detection were incubated with Alexa-488-conjugated secondary antibody (diluted in blocking solution) for 1 h. Finally, the preparations were washed three times in PBS, mounted in ProLong Gold antifade reagent (Invitrogen) containing 4′,6-diamidino-2-phenylindole (0.2 µg/ml). Slides for immunohistochemical detection were labeled using streptavidin–biotin–peroxidase method (LSAB Kit, Dako, France), washed with water and counterstained with hematoxylin (Sigma) for 20 s. The slides were then dehydrated by following the alcohol and xylene steps sequentially in a reverse order and finally mounted using a toluene-based mounting medium, (Protocol, Fisher Scientific, Houston, TX). Slides were finally observed using a Zeiss inverted microscope.

Fractionation of BLE using column chromatography with gradient elution

We employed column chromatography, a commonly used analytical technique to separate the constituents of betel leaves. Three grams of BLE was dissolved in methanol and adsorbed on silica gel (0.063–0.2 mm, 70–230 mesh) using a rotary evaporator. The column (3.5 cm × 45 cm) was filled with silica and the BLE–adsorbed silica mixture was added atop the silica followed by a layer of anhydrous sodium sulfate to remove any moisture. The column was then subjected to solvents of increasing polarity, the order being hexane < dichloromethane < ethyl acetate < methanol. The eluents were 100, 70, 50 and 30% hexane/ethyl acetate (500 ml each) followed by 500 ml of 10, 20, 30, 40 and 50% ethyl acetate/dichloromethane and 99.5, 99, 97, 95, 90 and 70% dichloromethane/methanol. The 15 fractions eluted were concentrated, and traces of solvents were removed by lyophilization and then subjected to TLC. Precoated alumina TLC silica gel 60 F_{254} plates were used and the spots were analyzed under UV light. Based on similar pattern and retention factors, the fractions were pooled together to finally yield 10 fractions.

Antiproliferative MTT assay

Cells were seeded in 96-well plates at a density of 3500 cells per plate. After 24 h of incubation, the medium was aspirated and replaced by media dosed with the drug at concentrations of 1, 10, 25, 50, 75, 100 and 250 µg/ml. Primary stocks were prepared by dissolving each fraction in DMSO at a concentration of 1 mg/ml. The secondary stock of each fraction was made at a concentration of 250 µg/ml followed by further dilutions. A total volume of 100 µl was added to each well. After 48 h of incubation, the drug-containing medium was aspirated and 100 µl of MTT (5 mg/ml) dye dissolved in RPMI was added. Following 4 h of incubation, the MTT dye was aspirated and the formazan crystals were solubilized in DMSO. Chromophoric groups in MTT (yellow) were reduced to a purple tetrazolium complex by viable cells and the absorbance was read at 570 nm using a SpectraMax Plus (Molecular Devices, Sunnyvale, CA) multiwell plate reader.

Identification of HC and EU by TLC

Each fraction obtained from column chromatography was spotted on a TLC plate (alumina TLC silica gel 60 F_{254}) along with the standards, HC and EU, and run through a series of solvent systems. The solvent systems used for TLC of various fractions were as follows: F1–F3—70:30 hexane/ethyl acetate; F4–F7—10:90 ethyl acetate/dicholoromethane; F8–F12—5:95 methanol/dicholoromethane; F13–F15—15:85 methanol/dicholoromethane. Once developed, the plates were screened for HC and EU by comparing the bands obtained for each fraction with the bands corresponding to the standards. The presence of HC and EU was confirmed by co-spotting the fraction with the standard compounds.

Subfractionation using preparative TLC

The individual constituents of BLE were further separated using preparative TLC method. One hundred milligrams of each fraction was loaded on the plate, a binary mobile phase of 30% ethyl acetate in hexane was used as the solvent system and the plate was developed in a glass chamber. The constituents separated as bands were scraped, dissolved in dichloromethane, filtered and concentrated for testing.

Identification of constituents by nuclear magnetic resonance

^{1}H NMR spectra were recorded on Bruker Avance (400 MHz) vertical bore spectrometer using 5 mm high-resolution probes, using $CDCl_3$, CD_3OD or DMSO-d_6 as solvent. Mass spectra (electrospray ionization mass spectrometry, positive ion mode) were recorded on a nanoLC-Q-TOF micro (Waters Micromass) mass spectrometer.

HPLC with UV and mass spectrometric detection

The HPLC-UV analysis of BLE was achieved on a HP 1100 series instrument (Agilent Technologies, Wilmington, DE) equipped with a photodiode array detector, using an Agilent XDB reversed phase (C-18, 1.8 µm, 4.6×50 mm, ODS-2) column. The mobile phase system consisting of solvent A (1.5% acetic acid in water) and solvent B (1.5% acetic acid in acetonitrile) was employed to achieve the separations. The gradient elution was set as follows: initial 8% solvent B for 5 min, achieving 20% solvent B at 60 min, which was held for an additional 5 min; this was followed by reconditioning to 8% B at 70 min and holding it for the next 5 min with a flow rate of 1 ml/min. Twenty microliters of BLE (1 mg/ml), dissolved and filtered in pure methanol, was injected into the system and the resultant HPLC-UV peaks were detected at 280 nm.

The HPLC-mass spectrometry (MS) analyses were performed in tandem with HPLC-UV using the same column interfaced to an Agilent 6400 Series Triple quadrupole LC/MS equipped with an electrospray ionization source, operable in both positive and negative ion modes. The nebulizer and collision gases were nitrogen and helium, respectively, with nitrogen set at 40 psi. A drying gas temperature of 300°C, drying gas flow rate of 9 l/min and capillary voltage of ±3000 V were the spray chamber specifications. The presence of HC (m/z = 151) in BLE was confirmed using MS-scan mode against pure standard.

Results

BLE inhibits human prostate tumors implanted in mice

Betel leaves have been shown to exhibit antiproliferative, antimicrobial and immunomodulatory properties. Considering the disease-fighting potential of BLE, we first examined its *in vivo* efficacy to inhibit human prostate tumor xenografts implanted subcutaneously in athymic nude mice. We used a stable PC-3 cell line that expresses luciferase (PC-3-luc), which enables real-time visualization and non-invasive monitoring of prostate cancer growth longitudinally in mice. In an experiment to determine the half-maximal lethal dose (LD_{50}),

we found that 700 mg/kg bw BLE was not well tolerated. Animals showed evident signs of discomfort and were thus euthanized at day 6. Next, we performed a dose-dependent study comprising five mice in each of four groups that were fed with vehicle (PBS) and 200, 400 or 650 mg/kg bw BLE daily by oral gavage for 6 weeks. Treatment responses were monitored twice a week by bioluminescent imaging (Figure 1A). Our data show that BLE-treated groups display inhibition of tumor growth significantly over 6 weeks in contrast to vehicle-treated control animals (Figure 1A and B). Relative photon quantitation revealed that 400 mg/kg bw BLE showed a ~61% inhibition in tumor volume at a confidence level of $P < 0.05$ ($n = 5$; Figure 1A), as measured at week 6 compared with vehicle-treated controls. Body weights were recorded twice a week to assess general health and well-being of animals during treatment. Mice in the BLE treatment groups exhibited normal weight gain with no signs of discomfort during the treatment regimen. All animals in the control group were euthanized by day 42 post-inoculation due to tumor overburden, in compliance with Institutional Animal Care and Use Committee guidelines. At the end of week 6, the excised tumors (Figure 1E) were weighed post-euthanasia, and a ~59% reduction in tumor weight was recorded in a subset of mice from 400 mg/kg bw BLE-treated group compared with controls. Though the 650 mg/kg bw BLE-fed group showed significant inhibition of tumor growth, mice could not tolerate the dose beyond 4 weeks of treatment (Figure 1Ai). These mice showed loss of appetite and weight and were euthanized at week 4.

The longevity of surviving mice in 400 mg/kg bw fed treatment group was monitored based on general health and well-being of the mice after BLE feeding was suspended at week 6. Kaplan–Meier analysis revealed that this treatment group exhibited 60% survival until 9 weeks (Figure 1D). Furthermore, biochemical analysis of serum markers (alanine transaminase, aspartate transaminase, alkaline phosphate, lactic acid dehydrogenase, creatinine kinase and urea nitrogen) was compared between the vehicle- and BLE-fed groups and was found to be within the normal range (Supplementary Figure 1, available at *Carcinogenesis* Online). The remarkable efficacy of BLE in inhibiting *in vivo* tumor growth encouraged us to determine the composition of this leaf extract to gain insights into its active principles.

BLE induces apoptosis and inhibits proliferation of tumor growth in vivo

Paraffin-embedded tumor tissue sections from vehicle- and BLE-fed mice were processed and immunostained for the cell proliferation marker, Ki67 (MIB-1), to evaluate *in vivo* inhibition of tumor growth. Our data showed a decrease in Ki67 expression in tumor sections from BLE-fed mice suggesting reduction in cell cycle activity upon BLE treatment (Figure 2Ai). Hematoxylin and eosin staining of tumor sections from BLE-fed mice revealed large pale pink cytoplasmic areas (Figure 2Aii) indicating clearing of tumor cells. Also, tumor sections from BLE-fed groups showed an increase in cleaved caspase-3 and cleaved poly (ADP ribose) polymerase expression (Figure 2Bi–Bii) compared with tumor sections from control vehicle-fed groups, implying induction of apoptosis upon BLE treatment.

Fractionation of BLE by column chromatography

The non-toxic *in vivo* attributes of BLE were also confirmed *in vitro*, wherein the half-maximal inhibitory concentration (IC_{50}) of BLE was found to be ~14-fold higher in normal prostate epithelial RWPE-1 cells (IC_{50} = 447 µg/ml, Supplementary Figure 2, available at *Carcinogenesis* Online) compared with human prostate cancer PC-3 cells (IC_{50}=32 µg/ml, Figure 3C and D). Given the wide therapeutic window, we next aimed to identify and isolate the bioactive constituent/s responsible for the *in vivo* efficacy of BLE. Thus, we first fractionated BLE using classical column chromatography by employing a gradient method to ensure absolute separation with a reduced analysis time. A series of solvent systems with a gradual increase in polarity were used to elute BLE along the silica gel column, and the separated constituents were collected as fractions (Figure 3A). Hexane (100%) was initially passed through the column to elute non-polar constituents of BLE. Ethyl acetate was then introduced into the mobile phase to enhance polarity along with dichloromethane, and elution of moderately polar constituents was thus achieved. Finally, increasing concentrations of methanol (from 0.5% up to 30%) in combination with dichloromethane were used to elute highly polar components (Figure 3A). Based on this separation scheme, BLE constituents were resolved into 15 fractions followed by subjection to analytical TLC. Fractions with comparable retention factor (R_f) values were pooled together to finally obtain 10 fractions, F1–F10 (Figure 3B), which were tested for their antiproliferative activity using an MTT assay in PC-3 cells. All fractions were concentrated under reduced pressure and lyophilized. While processing the first fraction, F1, no visible material was observed in the flask and thus this fraction could not be collected.

IC_{50} of nine fractions thus obtained are shown in Figure 3C and D. The least polar fraction, F2, was identified to be the most active with an IC_{50} of 10 µg/ml and showed a 3-fold better activity than the parent extract. The difference in the activity of various BLE fractions could be attributed to the presence of constituents varying in their polarity, which we attempted to investigate next.

Identification and quantitation of bioactive constituents of BLE

Several studies on piper betel leaves have reported that BLE is rich in phenols including HC, EU, chavibetol (CHV) and allylpyrocatechol (APC) (5,12,19). Chemically these compounds comprise monocyclic aromatic rings with phenolic and allyl moieties (20). Preliminary analysis of BLE fractions by TLC using HC and EU as standards (Figure 4A) revealed that F2 consisted of both EU and HC. However, TLC cannot rule out that the bands corresponding to EU and HC in F2 could be compounds with similar polarity including their positional isomers like CHV, isoeugenol and APC (12). Although EU was not seen in the later fractions, bands corresponding to HC were identified in F3 and F8–F10.

Further, co-spotting F2 with HC and EU confirmed the presence of bands corresponding to these pure standards. The next step was to examine the presence of HC and EU in all the fractions using UV detector equipped HPLC-UV coupled with tandem MS, an analytical technique with higher sensitivity and better separation efficiency. The HPLC-UV/MS analysis of F2–F10 in negative ion mode (scan, m/z = 100–500) revealed the presence of HC (m/z = 149) in all the BLE fractions. However, the abundance of HC in F2 was much higher compared with the rest of the fractions (Figure 4C). A linear decrease in its abundance was observed in the subsequent fractions and, interestingly, F10 was more concentrated in HC compared with F9. The rationale behind the 'bleed-over' of HC into later fractions could be attributed to the strength of intermolecular hydrogen bonds between the stationary silica and HC. With an increase in the polarity of the solvent system, the hydrogen bond breakage perhaps results in the spillover of some residual amounts into the later fractions, as detected in HPLC. Seemingly, the final fraction with the highest polarity perhaps completely solubilized the residue and thus HC was detectable in F10 as well. In addition, other phenolic compounds like chavicol (m/z = 133), phenylalanine (m/z = 164), HC acetate (m/z = 191), piperol A (m/z = 341) and piperol B (m/z = 355) were also detected in the BLE fractions. However, the molecular ion peak at m/z = 163 could not be confirmed as either EU or CHV. Given that the TLC and HPLC-MS data suggested the presence of HC and EU (Figure 4A and C) in F2, we next aimed at identifying the contribution of these individual phytochemicals toward F2's activity.

Subfractionation of F2

Bioactivity-guided fractionation of BLE suggested that F2 (IC_{50} = 10 µg/ml) is ~3-fold more active than BLE (IC_{50} = 32 µg/ml) in human prostate cancer PC-3 cells. We also tested the activity of F2 in other prostate cancer cell lines, namely, DU145 and 22RV1. The IC_{50} values of F2 in DU145 and 22RV1 were found to be 100 and 39 µg/ml, respectively (Figure 5A and B). Although the IC_{50} of F2 in

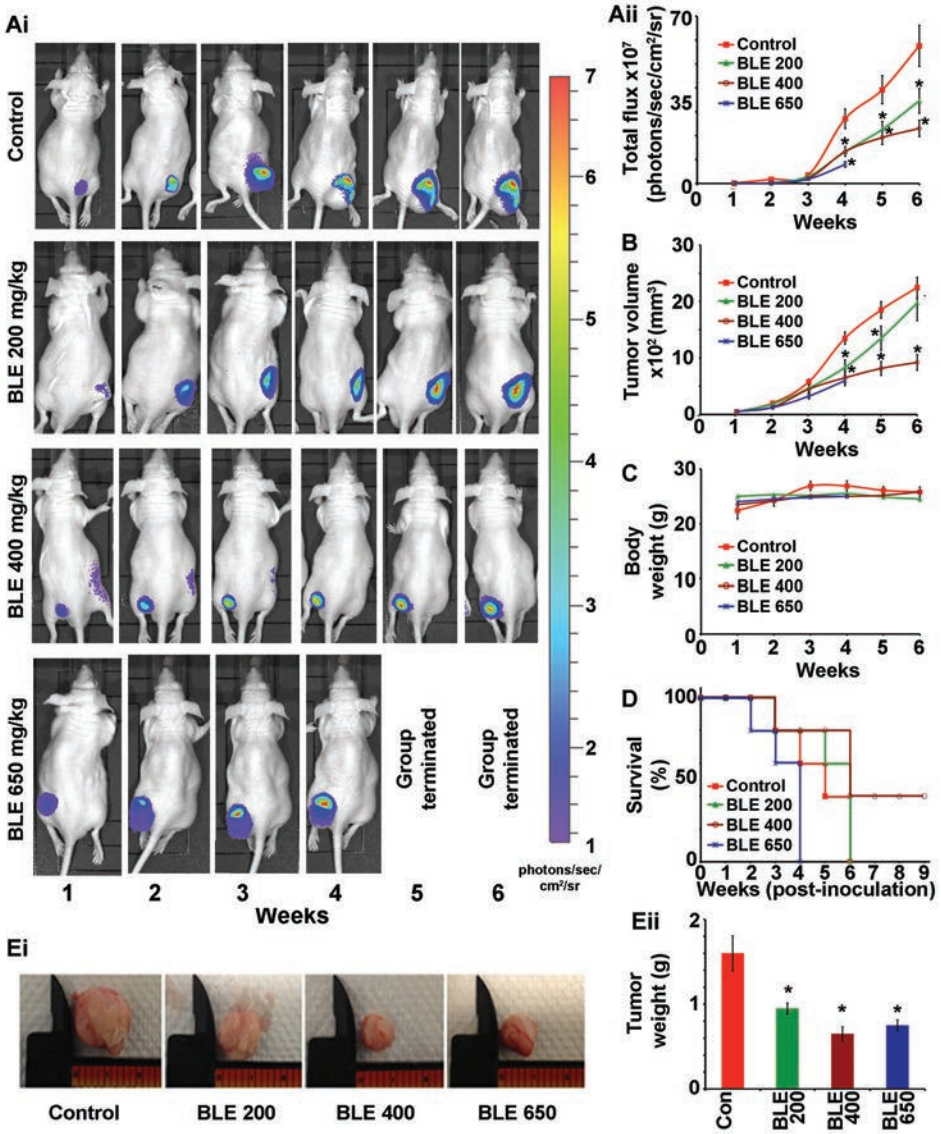

Fig. 1. Dietary feeding of BLE showed inhibition of human prostate tumor xenograft growth in nude mice. Male nude mice were subcutaneously injected with 10^6 PC-3-luc cells. (**Ai**) Bioluminescent images indicating progression of tumor growth of various dose groups over 6 weeks. (**Aii**) Graphical representation of photon quantitation from vehicle-treated mice and varying doses of BLE-treated mice for 6 weeks. (**B**) Tumor growth monitored by vernier calipers and presented as tumor volume in cubic millimeter, over a period of 6 weeks. (**C**) Graphical representation of body weight of vehicle-treated mice and varying doses of BLE-treated mice. (**D**) Survival graphs of BLE dose-dependent treatment and controls over 9 weeks. (**Ei**) Photographic images of excised tumors and (**Eii**) Graphical representation of tumor weight. The data points and the error bars represent average values and standard deviations, respectively, of all the animals in each group (*$P < 0.05$ compared with controls using two-sample *t*-test).

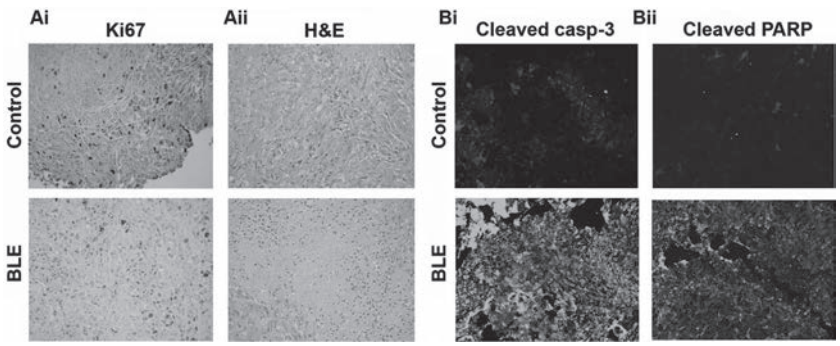

Fig. 2. (**Ai**) Ki67 immunostaining, (**Aii**) hematoxylin and eosin staining and immunofluorescent staining for apoptotic markers, (**Bi**) cleaved caspase-3 and (**Bii**) cleaved poly (ADP ribose) polymerase of tumor sections from vehicle- and BLE-fed mice.

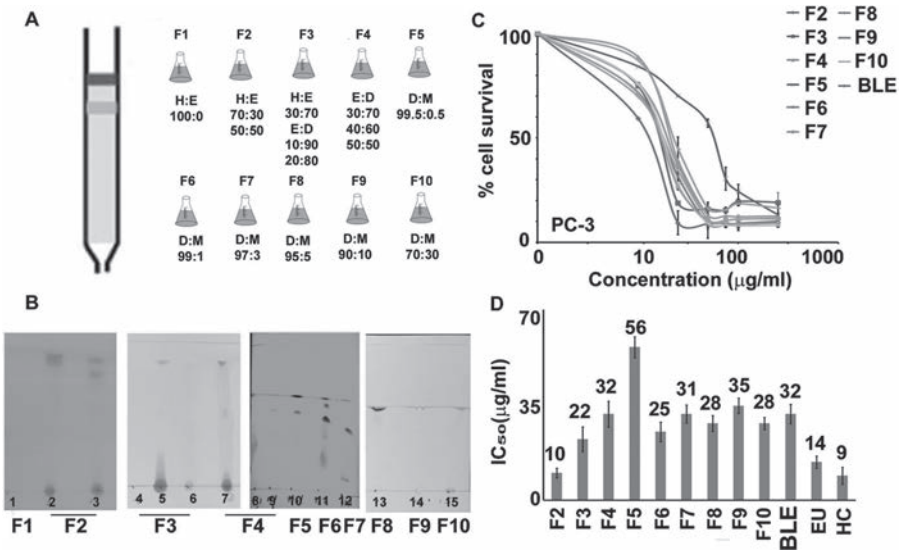

Fig. 3. Fractionation of BLE using column chromatography. (**A**) Ten fractions of BLE were obtained from classical chromatography using a gradient method. Fifteen fractions eluted were pooled to obtain 10 fractions based on comparable R_f values. H = hexane, E = ethyl acetate, D = dichloromethane and M = methanol. (**B**) TLC of 15 fractions using 70:30 hexane/ethyl acetate (1–3), 10:90 ethyl acetate/dichloromethane (4–7), 5:95 methanol/dichloromethane (8–12) and 15:85 methanol/dichloromethane (13–15) solvent systems. Fractions with comparable R_f values were pooled together to obtain 10 fractions. (**C**) Plot of percentage cell survival versus gradient concentration of different fractions. MTT assay was performed on fractions F2–F10 and compared with the parent BLE. (**D**) Bar graphical representation of IC_{50} of each fraction, parent BLE and the standards HC and EU. Data points and error bars represent average values and standard deviations, respectively, of three independent experiments ($P < 0.05$ compared with controls using two-sample *t*-test).

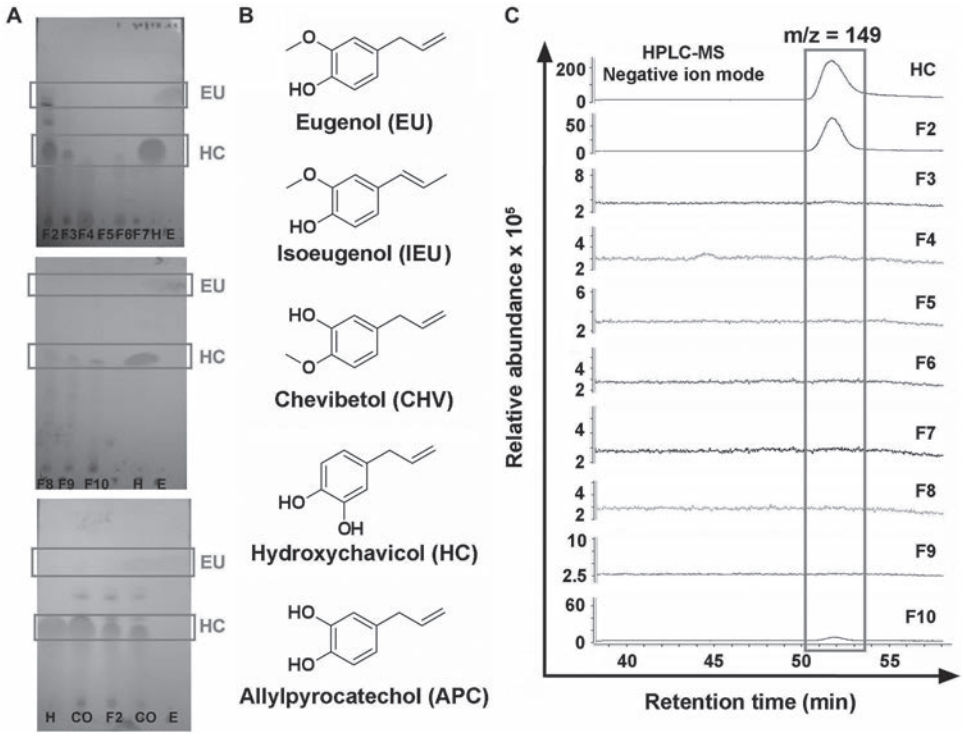

Fig. 4. Qualitative analysis of HC and EU. (**A**) TLC analysis was performed for each fraction and compared with the standards HC and EU. Comparable bands revealed that F2 contained both HC and EU. This was confirmed by co-spotting the fraction with each standard. (**B**) Chemical structures of polyphenols, EU with its positional isomers, isoeugenol and CHV, and HC with its positional isomer, APC. (**C**) LC-UV/MS comparison of HC in F2–F10. HC (m/z = 149) was detected in negative ion mode and was compared with the pure standard.

DU145 was 1.25-fold lower than that of BLE, 22RV1 showed only slightly lower IC_{50} of F2 compared with BLE (data not shown). Our results showed that F2's antiproliferative activity is in the following order: PC-3 > 22RV1 > DU145. PC-3 and DU145 cells are androgen-receptor negative and harbor non-functional p53, whereas 22RV1 cells are androgen-receptor positive and harbor wild-type p53. These data suggest that the antiproliferative activity was independent of androgen receptor or p53 status in the cell lines studied. Having compared the activity of F2 against different prostate cancer cell lines, our next step was to determine the bioactive constituents accountable for F2's activity.

The constituents of F2 were separated using preparative TLC by loading 100 mg of F2 onto the silica gel plate, followed by placing it

in a 70:30 hexane/ethyl acetate system. The most active fraction, F2, was resolved into six bands (Figure 5C), which were collected as subfractions (as mentioned in Materials and methods), and MTT assay was performed to determine their individual efficacies compared with the parent F2. The IC_{50} values for subfractions ranged between 16 and 251 µg/ml, with F2-2 through F2-6 showing similar potency as F2 (Figure 5D and E). F2-1, however, remained an exception and was found to be least active with an IC_{50} of 251 µg/ml (Figure 5E). The residual bands after initial loading of the sample onto the TLC plate could be due to various plant constituents like tannins and lignins, which did not move with the solvent system. The next step involved elucidation of chemical structure of the subfraction component/s.

Nuclear magnetic resonance and mass spectrometric characterization of F2 subfractions

Nuclear magnetic resonance (NMR) spectroscopy and tandem mass spectrometry (MS-MS) were employed for structural elucidation of F2 subfraction component/s. In addition, structure confirmation was also done by appropriate spectral comparisons with the information available in literature. Table I provides the NMR and MS data for F2-1 through F2-6. For F2-1, the molecular ion peak (Supplementary Figure 3, available at *Carcinogenesis* Online) corresponded to either EU acetate or CHV acetate, as both isomers show a molecular ion peak at 207 (molecular weight = 206). The F2-2 peaks in the NMR spectra (Supplementary Figure 4, available at *Carcinogenesis* Online) correspond to HC diacetate, and its molecular ion peak appears accurately at 235 (molecular weight = 234). The presence of molecular fragments of HC acetate and HC was detected in the mass spectrum. F2-3 (Supplementary Figure 5, available at *Carcinogenesis* Online) was identified to be HC diacetate. Two bands of the same constituent could be due to the presence of either ionized or other non-specific forms of intra- and intermolecular interactions. F2-4 (Supplementary Figure 6, available at *Carcinogenesis* Online) could not be identified, mostly due to the low amounts available; therefore, it remains an unknown in the current study. Our ongoing efforts are focused on a scale-up purification to identify F2-4. Also, spectral characterization and comparison with the standard identified F2-5 (Supplementary Figure 7, available at *Carcinogenesis* Online) as HC, with a molecular ion peak at 149 (molecular weight = 150). Furthermore, the spectrum did not show a triplet peak, thus ruling out the possibility of its

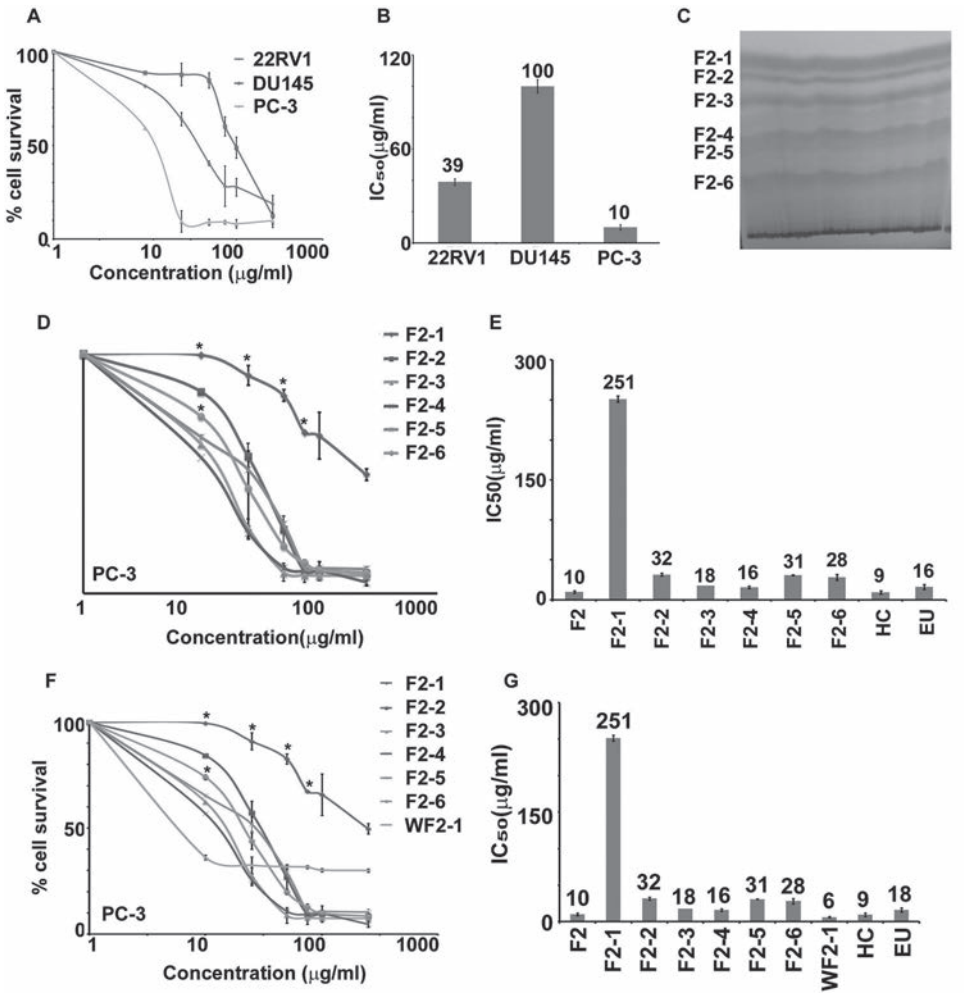

Fig. 5. Antiproliferative efficacy and subfractionation of F2. (**A**) Plot of cell survival versus concentration of F2 for different prostate cell lines. MTT assay was done on additional prostate cell lines, 22RV1 and DU145, to compare the efficacy of F2. (**B**) Bar graph represents IC_{50} of F2 for different prostate cancer cell lines DU145, 22RV1 and PC-3. (**C**) Preparative TLC was done to further separate the constituents of F2. The mobile phase was a binary mixture of 70:30 hexane/ethyl acetate. Six bands were obtained, which were scraped, reconstituted in dichloromethane, filtered and concentrated. (**D**) Plot of cell survival versus concentration of F2 subfractions for PC-3 cells using MTT assay (*$P < 0.09$ compared with controls using two-sample *t*-test). (**E**) Bar graph that compares the IC_{50} of F2 subfractions. Standards HC and EU were also tested for comparison. (**F**) Plot of cell survival versus concentration of F2 subfractions without F2-1. F2-1 (which demonstrated highest IC_{50}) was removed from F2 and the remaining fraction (WF2-1) was tested using PC-3 cells. WF2-1 stands for F2 without F2-1 (*$P < 0.09$ compared with controls using two-sample *t*-test). (**G**) Bar graph represents the IC_{50} of F2 subfractions including WF2-1. Standards HC and EU were also tested for comparison.

Table I. Composition of F2 subfraction

Subfraction	Constituent/s
F2-1	CHV acetate/EU acetate
^{1}H NMR ($CDCl_3$) δ7.03 (q, 1H, *J* = 8.0 Hz), 6.91 (m, 2H), 5.95 (m, 1H, *J* = 8.0 Hz), 5.09 (t, 2H, *J* = 8.0 Hz), 3.83 (s, 3H), 3.34 (d, 2H, *J* = 8.0Hz), 2.32 (s, 3H) MS (+): calcd for $C_{12}H_{14}O_3$, 206.2; found, 207.1 $[M + H]^+$	
F2-2	HC diacetate
^{1}H NMR ($CDCl_3$) δ7.01 (s, 1H), 7.10 (m, 2H, *J* = 8.0 Hz), 5.95 (m, 1H), 3.40 (d, 2H, *J* = 8.0 Hz), 2.29 (s, 6H), 3.34 (d, 2H, *J* = 8.0 Hz), 2.32 (s, 3H) MS (+): calcd for $C_{13}H_{14}O_4$, 234.2; found, 257.0 $[M + Na]^+$	
F2-3	HC diacetate
^{1}H NMR ($CDCl_3$) δ7.01 (s, 1H), 7.10 (m, 2H, *J* = 8.0 Hz), 5.95 (m, 1H), 3.40 (d, 2H, *J* = 8.0 Hz), 2.29 (s, 6H), 3.34 (d, 2H, *J* = 8.0Hz), 2.32 (s, 3H) MS (+): calcd for $C_{13}H_{14}O_4$, 234.2; found, 257.0 $[M + Na]^+$	
F2-4	Unknown
F2-5	HC
^{1}H NMR ($CDCl_3$) δ6.80 (d, 1H, *J* = 8.0 MHz), 6.72 (s, 1H), 6.64 (d, 2H, *J* = 8.0 Hz), 5.95 (m, 2=1H), 5.10 (br, OH), 3.29 (d, 2H, *J* = 8.0 Hz) MS (+): calcd for $C_9H_{10}O_2$, 150.0; found, 151.0 $[M + H]^+$	
F2-6	Unknown

positional isomer APC. The structure of F2-6 is still unidentified and will be a subject of future studies (Supplementary Figure 8, available at *Carcinogenesis* Online).

Identification of F2-1 composition

Having analyzed the distinct activity of each subfraction, we found that the IC_{50} of F2-1 was quite high (251 µg/ml) compared with other subfractions. To correlate its contribution to F2's efficacy, all subfractions excluding F2-1 were combined and tested in PC-3 cells (Figure 5F). The resultant IC_{50} value of this mixture was 6 µg/ml (Figure 5G), which was comparable with F2's activity as a whole, thus revealing that F2-1 was not vital for F2's activity. However, as the NMR and MS data (Supplementary Figure 9, available at *Carcinogenesis* Online) suggested an ambiguity regarding the identity of F2-1, coupled with our initial observations of EU's presence in F2 (Figure 4A), it was important to confirm the identity of F2-1.

To gain deeper insights into F2-1's identity, ^{13}C NMR analysis was performed (Supplementary Figure 9, available at *Carcinogenesis* Online), which revealed that F2-1 was CHV acetate. Comparing the initial TLC data (Figure 4A) and the corresponding IC_{50} values (Figure 3C and D) of all BLE fractions, we rationalized that HC seemed to play a major role in imparting BLE's *in vitro* and *in vivo* efficacy.

Determining the contribution of HC to BLE's antiproliferative activity

The HPLC analysis of BLE fractions revealed traces of HC in F4–F10 (Figure 4C). Comparing the efficacy of F2 with that of F4–F10 fractions (Figure 3C and D), we reasoned that HC could be majorly responsible for F2's efficacy. To confirm this further, the low-abundance HC fractions, i.e. F4–F10, were combined and tested in comparison with F2, which had the highest abundance of HC. The resultant efficacy of F4–F10 mixture (25.11 µg/ml) was lower than that of F2 (10 µg/ml) (Figure 6A and B), thus supporting a major role of HC in F2's efficacy. Though the contributions of other phytochemicals cannot be discounted as they might be offering synergy, HC appears to be majorly responsible for F2's activity. Thus, our data suggest that HC might be the major contributor to BLE's antiproliferative efficacy among all the other constituents.

Quantitation of HC in BLE by HPLC

Next, to determine the presence of HC in BLE, HPLC-UV and HPLC-MS analyses were employed simultaneously in the negative ion mode using acetonitrile:H_2O (1.5% acetic acid) solvent system. BLE (1 mg/ml) dissolved in pure methanol was injected into the system and the tandem mass spectrum thus obtained was scanned for a *m*/*z* range of 100–500. A significant peak was detected with an *m*/*z* of 149, matching that of HC as described previously (Figure 6C). Quantitation of HC was carried out by calibration of a standard curve with known concentrations of pure HC, followed by calculating the abundance of HC in BLE. This analysis indicated that HC was present at ~26.59% in BLE. Interestingly, F2 contained ~25.25% of HC, thus implying that ~95% of the total HC content of BLE was reconstituted in F2. Further, when tested for its antiproliferative activity, F2 was found to be 3-fold more active than BLE, suggesting the usefulness of HC isolation from betel leaves to evaluate it as a single agent for prostate cancer management.

Discussion

Extensive literature suggest that fruits, vegetables and spices impart several health benefits and are thus regarded as potential chemopreventive agents (2,4,8,21). It has been widely appreciated that fruits and vegetables, with their complex array of phytochemicals, alter the progression of deadly neoplasms, particularly slow-growing prostate cancers (2,3,11,22). Betel leaf is traditionally used as a mouth freshener in India and China. Consumed regularly by nearly 600 million people in Asia, these leaves are a focus of intense research due to their wide repertoire of medicinal properties (17,18). Our current study reports the beneficial effects of betel leaves both *in vivo* and *in vitro* in prostate cancer models. We found that oral feeding of 400 mg/kg bw BLE is quite effective in tumor growth inhibition with no detectable toxicity compared with vehicle-treated controls and other doses employed in the current study (Figure 1). This is in concordance with a similar study where BLE significantly inhibited 7,12-dimethylbenz(a) anthracene-induced skin tumors in swiss mice (23).

Plant extracts, as a natural blend of phytochemicals, offer immense opportunities for discovery of active constituents, an archetype of current pharmaceutical industries (24). Classic examples include isolation of vinca alkaloids like vinblastine and vincristine from leaves of *Catharanthus roseus* and taxol from the bark of yew tree (25,26). These drugs are currently extensively used for a variety of neoplasms in the clinic (23). Fractionation using classical chromatography has been widely used for isolation of active ingredients from plant extracts (10,27). Several plant phytochemicals have been extracted and isolated employing a bioactivity-guided approach. For example, fraction F2 obtained from the methanolic extract of *Smilax spinosa*, an ethnopharmaceutical remedy, displayed a higher proapoptotic activity than the crude extract (28). Also, it has been reported that the procyanidin-rich fractions obtained from apple juice exhibit radical scavenging properties and have shown to be more efficacious than the apple juice extract itself (29). On similar lines of thought, we fractionated BLE into 10 fractions based on their TLC profiles (Figure 3A and B). Further, the most active fraction was identified (Figure 3C and D) and its active ingredient, HC, was qualitatively and quantitatively characterized using preparative TLC, NMR and HPLC (Figure 5C, Supplementary Figure 7, available at *Carcinogenesis* Online and Figure 6C, respectively).

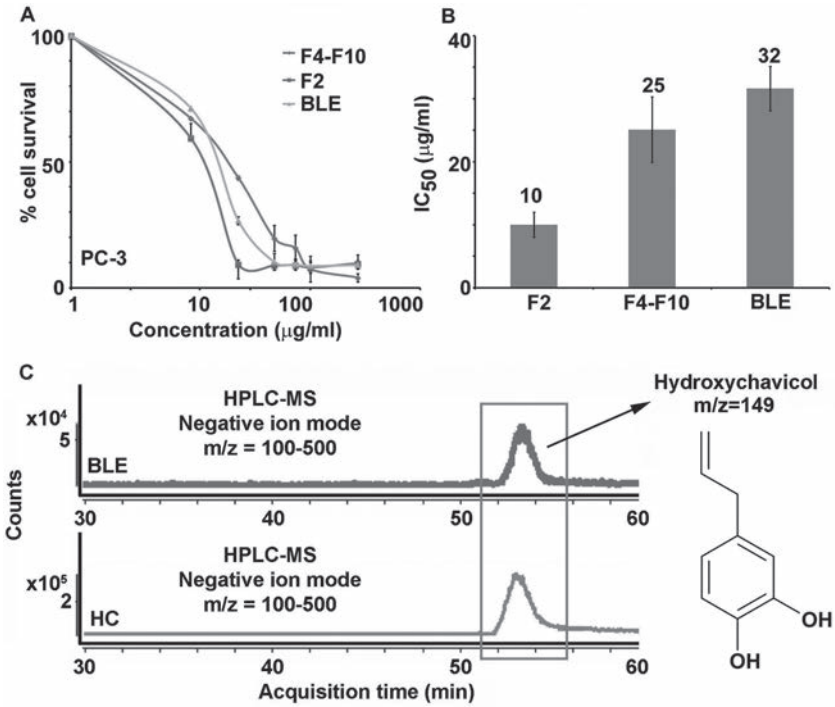

Fig. 6. Comparison between F2 and combined fractions F4–F10. (**A**) Line plot of cell survival versus gradient concentrations for F2, F4–F10 and BLE ($P < 0.05$ compared with controls using two-sample *t*-test). (**B**) Bar graphical representation of the IC_{50} values of F2, F4–F10 and BLE. (**C**) HPLC-MS analysis for identification and quantitation of HC in BLE.

Several studies suggest that the synergistic effect of constituent phytochemicals is responsible for the efficacy of whole plant extracts (30,31). Although the concept of synergistic interrelationships between complex phytochemicals explains the superior activity of several foods compared with their constituents, isolation of the single constituent is favored over complex mixtures when the bulk of activity resides in a single ingredient. It is likely that such complex mixtures may contain additional pigments and polyphenols, which may antagonize the efficacy of the active ingredient (32). In addition, the abundance of constituent phytochemicals in whole foods may vary due to factors like climate, location and physical and chemical stimuli (32). This is exemplified by a recent study, which reported that the polyphenolic content of a green tea infusion varied with cultivation and the technique of brewing, as an unstandardized infusion with a low dose of active principles, did not display the expected results in clinical trials and was thus withdrawn from future studies (11). On similar lines, a comparative report exists on three different varieties of *P.betel* (Bangla, Sweet and Mysore), which suggests that the Bangla variety exhibits the best antioxidant activity with the highest polyphenolic content. The other two varieties with reduced polyphenol content were effective at much higher concentrations (12). Given that several varieties including hybrids are increasingly being cultivated all over the world, it is practically difficult to draw generalizations on the efficacy of these different varieties of betel leaves that differ in their variety and geographical location.

We observed that upon fractionation of BLE, F2 constituted ~95% of BLE's total HC content (Figure 6C) and also exhibited improved efficacy as compared with the parent (Figure 3C and D). A study comparing the activity of BLEs made in various solvents supports our observation, wherein the extract with highest amount of HC displayed superior antioxidant activity (20). Additionally, the relevance of an optimal composition of phytochemicals for maximum therapeutic efficacy has been widely reported in the literature supporting our observations (22,29–31,33–37). Furthermore, HC has been shown to induce apoptosis in leukemic cells by increasing the levels of mitochondria-derived reactive oxygen species that activated the c-jun N-terminal kinase pathway, thus leading to the loss of mitochondrial membrane potential (19). It has also been shown to deplete cellular glutathione levels, leading to oxidative stress (38). These mechanisms might contribute to the low IC_{50} value of BLE as observed in our study. Although other BLE components like CHV have demonstrated radical scavenging, antilipid peroxidation and radioprotective properties, our observations suggest that their contribution toward BLE's activity is insignificant. This could also be attributed to the diverse chemistry and biology of these compounds, as the effects of an electron-donating moiety are likely to vary depending upon its nature and position on the phenol ring. The presence of a hydroxyl group, an electron-donating moiety at the ortho and para positions, enhances its reducing property. For example, the methylated phenol, CHV, lacks this free catechol, which might result in its lower antioxidant potential. This may better explain the enhanced activity of HC, a phenol with a free catechol group, compared with CHV (12).

Furthermore, several isolated compounds of plant origin, like HC in our case, have proven to be advantageous, as they also set grounds for chemical modifications and rational drug discovery for enhanced efficacy and superior pharmacological profiles. For example, artemesisin (an antimalarial drug derived from the medicinal herb *Artemisia annua*) was chemically modified to sodium artesunate, which displayed higher solubility and hence ease of administration (39). On similar grounds, the most active classes of anticancer drugs, like vincas and taxanes, have all been subjected to extensive structure–activity studies to generate superior analogs that have been reported to be effective cancer cell death traps (40,41). These agents not only portend significantly greater tumor growth inhibiting activity but also are known for their reduced toxicity as compared with their founding molecules. More recent advances in anticancer therapeutics highlight the advent of noscapine analogs as 'kinder and gentler' microtubule modulating agents (42–44) that perhaps are relatively non-toxic compared with the classical antimicrotubule agents that impart toxicity to normal cells.

Thus, we envision that in scenarios where a single component, such as HC from betel leaves, monopolizes the bioactivity compared with other constituents, it may be beneficial to extract the most active constituent and optimize its therapeutic concentrations

and pharmacokinetic profile that renders maximum bioavailability to achieve superior therapeutic indices. Given the significant contribution of HC toward BLE's activity, we strongly believe that isolating HC from the BLE plant matrix opens new windows to unveil its mechanisms of anticancer action.

Supplementary material

Supplementary Figures 1–10 can be found at http://carcin.oxfordjournals.org/.

Funding

This work was supported by ACS grant (Award #: 121728-RSG-12-004-01-CNE) to R.A. from the American Cancer Society.

Conflict of Interest Statement: None declared.

References

1. Parkin,D.M. *et al.* (2005) Global cancer statistics, 2002. *CA Cancer J. Clin.*, **55**, 74–108.
2. Shukla,S. *et al.* (2005) Dietary agents in the chemoprevention of prostate cancer. *Nutr. Cancer*, **53**, 18–32.
3. Chan,R. *et al.* (2009) Prostate cancer and vegetable consumption. *Mol. Nutr. Food Res.*, **53**, 201–216.
4. Cooke,D. *et al.* (2005) Anthocyans from fruits and vegetables—does bright colour signal cancer chemopreventive activity? *Eur. J. Cancer*, **41**, 1931–1940.
5. Kaur,M. *et al.* (2009) Anticancer and cancer chemopreventive potential of grape seed extract and other grape-based products. *J. Nutr.*, **139**, 1806S–1812S.
6. Yang,C.S. *et al.* (2001) Inhibition of carcinogenesis by dietary polyphenolic compounds. *Annu. Rev. Nutr.*, **21**, 381–406.
7. Craig,W.J. (1999) Health-promoting properties of common herbs. *Am. J. Clin. Nutr.*, **70**, 491S–499S.
8. Surh,Y.J. (2003) Cancer chemoprevention with dietary phytochemicals. *Nat. Rev. Cancer*, **3**, 768–780.
9. Quideau,S. *et al.* (2011) Plant polyphenols: chemical properties, biological activities, and synthesis. *Angew. Chem. Int. Ed. Engl.*, **50**, 586–621.
10. Sasidharan,S. *et al.* (2011) Extraction, isolation and characterization of bioactive compounds from plants' extracts. *Afr. J. Tradit. Complement. Altern. Med.*, **8**, 1–10.
11. Johnson,J.J. *et al.* (2010) Green tea polyphenols for prostate cancer chemoprevention: a translational perspective. *Phytomedicine*, **17**, 3–13.
12. Rathee,J.S. *et al.* (2006) Antioxidant activity of piper betel leaf extract and its constituents. *J. Agric. Food Chem.*, **54**, 9046–9054.
13. Kunnumakkara,A.B. *et al.* (2008) Curcumin inhibits proliferation, invasion, angiogenesis and metastasis of different cancers through interaction with multiple cell signaling proteins. *Cancer Lett.*, **269**, 199–225.
14. Sung,B. *et al.* (2012) Cancer cell signaling pathways targeted by spice-derived nutraceuticals. *Nutr. Cancer*, **64**, 173–197.
15. Bhide,S.V. *et al.* (1991) Chemopreventive efficacy of a betel leaf extract against benzo[a]pyrene-induced forestomach tumors in mice. *J. Ethnopharmacol.*, **34**, 207–213.
16. Bhattacharya,S. *et al.* (2005) Radioprotective property of the ethanolic extract of Piper betel leaf. *J. Radiat. Res.*, **46**, 165–171.
17. Bajpai,V. *et al.* (2010) Profiling of *Piper betel* Linn. cultivars by direct analysis in real time mass spectrometric technique. *Biomed. Chromatogr.*, **24**, 1283–1286.
18. Kumar,N. (2010) *Piper betel* Linn. a maligned Pan-Asiatic plant with an array of pharmacological activities and prospects for drug discovery. *Curr. Sci.*, **99**, 922–932.
19. Chakraborty,J.B. *et al.* (2012) Hydroxychavicol, a Piper betel leaf component, induces apoptosis of CML cells through mitochondrial reactive oxygen species-dependent JNK and endothelial nitric oxide synthase activation and overrides imatinib resistance. *Cancer Sci.*, **103**, 88–99.
20. Pin,K.Y. (2010) Antioxidant and anti-inflammatory activities of extracts of betel leaves (*Piper betel*) from solvents with different polarities. *J. Trop. Forest Sci.*, **22**, 448–455.
21. Chu,Y.F. *et al.* (2002) Antioxidant and antiproliferative activities of common vegetables. *J. Agric. Food Chem.*, **50**, 6910–6916.
22. Veluri,R. *et al.* (2006) Fractionation of grape seed extract and identification of gallic acid as one of the major active constituents causing growth inhibition and apoptotic death of DU145 human prostate carcinoma cells. *Carcinogenesis*, **27**, 1445–1453.
23. Azuine,M.A. *et al.* (1991) Chemopreventive efficacy of betel leaf extract and its constituents on 7,12-dimethylbenz(a)anthracene induced carcinogenesis and their effect on drug detoxification system in mouse skin. *Indian J. Exp. Biol.*, **29**, 346–351.
24. Rasoanaivo,P. *et al.* (2011) Whole plant extracts versus single compounds for the treatment of malaria: synergy and positive interactions. *Malar. J.*, **10** (suppl. 1), S4.
25. Noble,R.L. (1990) The discovery of the vinca alkaloids—chemotherapeutic agents against cancer. *Biochem. Cell Biol.*, **68**, 1344–1351.
26. Hule,C.W. (2002) A review of modern sample-preparation techniques for the extraction and analysis of medicinal plants. *Anal. Bioanal. Chem.*, **373**, 23–30.
27. Dinan,L. *et al.* (2001) Chromatographic procedures for the isolation of plant steroids. *J. Chromatogr. A*, **935**, 105–123.
28. Seelinger,M. *et al.* (2012) Methanol extract of the ethnopharmaceutical remedy *Smilax spinosa* exhibits anti-neoplastic activity. *Int. J. Oncol.*, **41**, 1164–1172.
29. Zessner,H. *et al.* (2008) Fractionation of polyphenol-enriched apple juice extracts to identify constituents with cancer chemopreventive potential. *Mol. Nutr. Food Res.*, **52** (suppl. 1), S28–S44.
30. Jacobs,D.R. Jr *et al.* (2009) Food synergy: an operational concept for understanding nutrition. *Am. J. Clin. Nutr.*, **89**, 1543S–1548S.
31. Wagner,H. (2011) Synergy research: approaching a new generation of phytopharmaceuticals. *Fitoterapia*, **82**, 34–37.
32. Raskin,I. *et al.* (2002) Plants and human health in the twenty-first century. *Trends Biotechnol.*, **20**, 522–531.
33. Ferguson,P.J. *et al.* (2004) A flavonoid fraction from cranberry extract inhibits proliferation of human tumor cell lines. *J. Nutr.*, **134**, 1529–1535.
34. Zhao,J. *et al.* (1999) Anti-tumor-promoting activity of a polyphenolic fraction isolated from grape seeds in the mouse skin two-stage initiation-promotion protocol and identification of procyanidin B5-3′-gallate as the most effective antioxidant constituent. *Carcinogenesis*, **20**, 1737–1745.
35. Miura,T. *et al.* (2008) Apple procyanidins induce tumor cell apoptosis through mitochondrial pathway activation of caspase-3. *Carcinogenesis*, **29**, 585–593.
36. Toi,M. *et al.* (2003) Preliminary studies on the anti-angiogenic potential of pomegranate fractions *in vitro* and *in vivo*. *Angiogenesis*, **6**, 121–128.
37. Kandil,F.E. *et al.* (2002) Composition of a chemopreventive proanthocyanidin-rich fraction from cranberry fruits responsible for the inhibition of 12-O-tetradecanoyl phorbol-13-acetate (TPA)-induced ornithine decarboxylase (ODC) activity. *J. Agric. Food Chem.*, **50**, 1063–1069.
38. Jeng,J.H. *et al.* (2004) Reactive oxygen species are crucial for hydroxychavicol toxicity toward KB epithelial cells. *Cell. Mol. Life Sci.*, **61**, 83–96.
39. Houghton,P.J. (1995) The role of plants in traditional medicine and current therapy. *J. Altern. Complement. Med.*, **1**, 131–143.
40. Ranaivoson,F.M. *et al.* (2012) Structural plasticity of tubulin assembly probed by vinca-domain ligands. *Acta Crystallogr. D Biol. Crystallogr.*, **68**, 927–934.
41. Fauzee,N.J. *et al.* (2012) Novel hydrophilic taxane analogues inhibit growth of cancer cells. *Asian Pac. J. Cancer Prev.*, **13**, 563–567.
42. Pannu,V. *et al.* (2012) Induction of robust *de novo* centrosome amplification, high-grade spindle multipolarity and metaphase catastrophe: a novel chemotherapeutic approach. *Cell Death Dis.*, **3**, e346.
43. Zhou,J. *et al.* (2003) Brominated derivatives of noscapine are potent microtubule-interfering agents that perturb mitosis and inhibit cell proliferation. *Mol. Pharmacol.*, **63**, 799–807.
44. Jaiswal,A.S. *et al.* (2009) 9-Bromonoscapine-induced mitotic arrest of cigarette smoke condensate-transformed breast epithelial cells. *J. Cell. Biochem.*, **106**, 1146–1156.

Received September 12, 2012; revised February 4, 2013; accepted February 13, 2013